Journal of Power Sources 196 (2011) 8494–8499

Contents lists available at ScienceDirect

Journal of Power Sources

journal homepage: www.elsevier.com/locate/jpowsour

Carbon nanofibers improve both the electronic and ionic contributions of the electrochemical performance of composite electrodes

C. Fongy [b], S. Jouanneau [b], D. Guyomard [a], B. Lestriez [a,*]

[a] Institut des Matériaux Jean Rouxel (IMN), Université de Nantes, CNRS, 44322 Nantes Cedex 3, France
[b] Laboratoire des Composants pour l'Energie, CEA, F-38054 Grenoble, France

ARTICLE INFO

Article history:
Received 21 March 2011
Received in revised form 20 April 2011
Accepted 3 June 2011
Available online 12 June 2011

Keywords:
Composite electrode
Conductive additive
$LiFePO_4$
Carbon nanofibre

ABSTRACT

The impact of carbon nanofibers as conductive additive on the electrochemical performance of a $LiFePO_4$-based composite electrode for lithium battery is investigated here. We use a new method that allows discriminating between the electronic and the ionic wirings contributions to the polarization and the specific capacity at different discharge rates [C. Fongy, et al., J. Electrochem. Soc., 157 (2010) A885; C. Fongy, et al., J. Electrochem. Soc., 157 (2010) A1347]. Results show this conductive additive is not only beneficial in terms of electronic wiring but it also enables to reach better high rate performance by improving the ionic wiring as it decreases the tortuosity of the porosity within the composite electrode architecture.

1. Introduction

Carbon nanofibers (CNF) have been introduced in the formulation of both the negative [1–3] and the positive [4–6] composite electrodes for lithium batteries as a conductive additive since a few years. It has been observed that CNF improve the electrical conductivity, the rate performance and the cyclability of the composite electrodes [1–5]. Improved performance compared to the usual conductive additive, namely carbon black (CB) or graphite (G), is attributed to their higher electronic conductivity due to their high aspect ratio and high crystallinity. Due to their fibrous shape, CNF form long-range resilient conductive bridges which favor a faster, durable and more uniform distribution of electrons to the active mass in the composite electrode [1–5]. Generally, using a blend of CNF with CB or G results in optimal performance with a minimum amount of these additives into the composite electrode formulation [4,5]. Blending conductive additives allows to realize the compromise between: (i) a low percolation threshold, which can be achieved thanks to the high aspect ratio of the CNF [7] and (ii) a high number of contacts between the conductive additive network and the active electrode particles, mandatory condition to reach a low electrode resistance [8–10] which is typically achieved by using well dispersed CB nanoparticles [11–13].

The electrochemical performance, however, depends on both the electronic and ionic conductivity of the composite electrode. We recently proposed an experimental method to discriminate between these both types of limitations [14,15]. This method is used here to show that CNF not only improve the electronic wiring of the composite electrode but also the ionic one. The introduction of CNF in the composite electrode decreases the mean pores tortuosity, by creating linear paths for lithium diffusion along their surfaces, which results in a sensitive improvement of the ionic conductivity.

2. Background

Our recent method to analyze the electrode performance [14,15] uses a set of easy-handling Eqs. (1)–(3) relate the specific capacity Q (mAh g^{-1}), the specific current I_m (mA g^{-1}), and the equilibrium discharge capacity Q_0 extrapolated at very low specific current. Q_0 depends on the fraction of active material (AM) grains truly connected to both the electronic and ionic wires of the composite electrode. Q depends on Q_0 and I_m through the rate factor k, that has unit of a time and quantifies the diminution of the discharge capacity with the increasing currents.

$$Q = Q_0 - kI_m \quad (1)$$

Another way of writing Eq. (1) is

$$Q = I_m \left(\frac{Q_0}{I_m} - k \right) \quad (2)$$

* Corresponding author. Tel.: +33 2 4 03 739 32; fax: +33 2 40 37 39 95.
E-mail address: bernard.lestriez@cnrs-imn.fr (B. Lestriez).

0378-7753/$ – see front matter © 2011 Elsevier B.V. All rights reserved.
doi:10.1016/j.jpowsour.2011.06.022

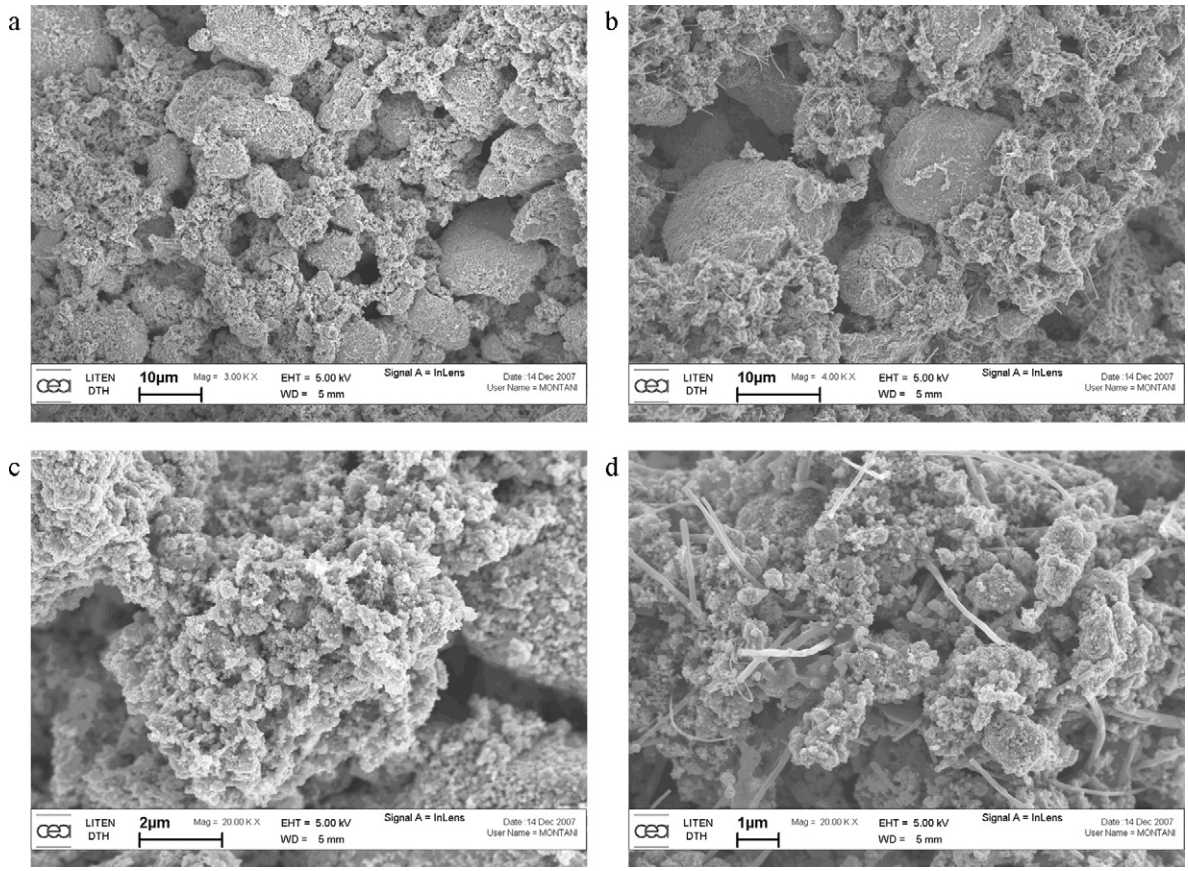

Fig. 1. SEM observations of non-densified $LiFePO_4$-based composite electrode (a and c) without or (b and d) with CNF.

where Q_0/I_m represents the discharge duration to get the total capacity of the electrode. When Q_0/I_m is the order of k the capacity delivered by the electrode drops to zero. This way, k can be seen as a time constant measuring the kinetics of the composite electrode. The lower is k, the faster is the electrode and the more power is delivered by the electrode. k is a rate limitation factor. The general expression of k is

$$k = k_{ionic} + k_e + k_{AM} \tag{3}$$

with (i) k_{AM} the active material limitation (solid-state mass transport diffusion time); (ii) k_{ionic} the ionic wires limitation; (iii) k_e the electronic wires limitation [14]. Expressions for k_{AM} and k_{ionic} are

$$k_{AM} = \frac{4r}{D_{AM}\pi^2 A\rho} \tag{4}$$

where r is the solid-state mass transport distance (the particles radius when Q reaches Q_0), D_{AM} is the apparent lithium diffusion coefficient in the active material, A is the surface area available for lithium insertion ($m^2\,g^{-1}$) and ρ is the active material density ($g\,cm^{-3}$). Note that this formula is general and takes into account the anisotropy of the Li^+ ion mobility into the active material structure. Also note that the electronic transport properties of the active material do not appear explicitly in this formula, but it is well known that ionic and electronic motions are strongly correlated in any insertion material.

$$k_{ionic} = \frac{L^2}{3D_0\varepsilon^\alpha} \tag{5}$$

with the electrode thickness L, the electrode porosity ε and tortuosity α, and the liquid electrolyte diffusion coefficient D_0. One can see that the expression for k_{ionic} is close to the one for the mean time for lithium diffusion if Brownian motions are considered. Unfortunately, to date no expression has been found for k_e. With increasing the current rate, k is observed to decrease, meaning that the composite electrode appears electrochemically faster at high rate than at low rate, a non-intuitive feature we attributed to an increase of the active material conductivity with increasing current density [14]. Another interpretation is the following. When increasing the current rate, the mean distance over which the charges (Li^+ and e^-) are transported into the bulk of the active material is shorter than the particles radius, thus resulting in a decrease of the active material limitation k_{AM} according to Eq. (4).

We also analyze the electrode polarization resistance through

$$E_0 - E = I(R_{AM} + R_W + xR_x) \tag{6}$$

where E_0 is the theoretical voltage of the electrode (3.45 V for $LiFePO_4$), E is the operating voltage, I is the current, x is the insertion degree of Li in Li_xFePO_4 ($0 \le x \le 1$). R_{AM} is the contribution of the AM and R_W stands for the contribution of the electronic wires to the electrode polarization resistance at zero insertion and thus characterizes the better-connected AM grains. The sum $R_{AM} + R_W$ determines the value of the potential plateau extrapolated at zero insertion, while R_x takes into consideration its slope in the voltage–composition curve to determine the potential at a given insertion value. R_x is sensitive to the distribution of electronic and ionic wirings of the AM grains which are poorly connected to the electronic and ionic percolating networks of the electrode and react at lower potential due to increased polarization. R_x is dependent on the rate. The expression of R_{AM} was given by Gaberscek and co-workers [8], and R_{AM} was shown to vary inversely with the active mass loading [8,15]. Thus, the study of the variation of the electrode polarization resistance (equal to $R_{AM} + R_w$, at $x = 0$) as a

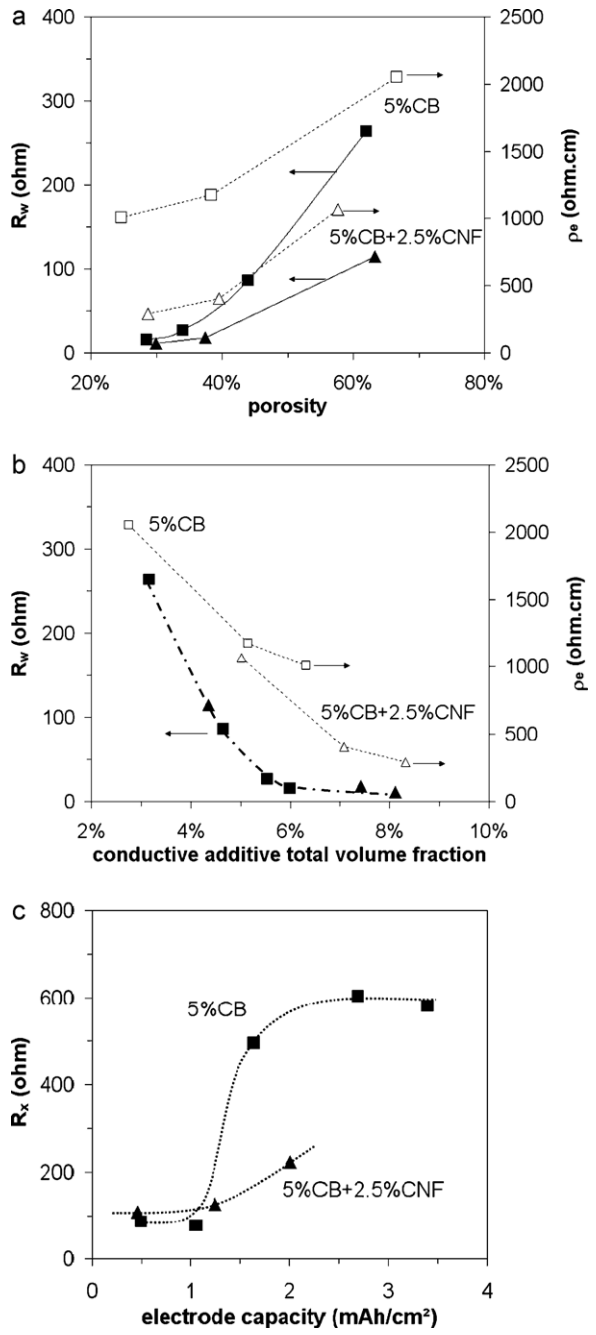

Fig. 2. (a) R_w (full symbols) and electronic resistivity ρ_e (open symbols) as functions of the electrode porosity for 1.8 mAh cm^{-2} electrodes containing 5 wt% (■-, □) or 7.5 wt% (▲, △) of conductive additives. (b) R_w (full symbols) and electronic resistivity ρ_e (open symbols) as functions of the conductive additive total volume fraction. (c) R_x as a function of the electrode capacity for electrodes containing 5 wt% (■) or 7.5 wt% (▲) of conductive additives – 2*C*-rate – 30–35% of porosity.

function of the active mass loading gives R_w, independent of the rate.

All the parameters in Eqs. (1)–(6) allow quantifying the electronic and ionic wires role in the electrochemical performance depending on the electrode loading and composition, and depending on the discharge rate. The $LiFePO_4$ based electrodes studied in this paper only differ in their mix of conductive additives used: 5 wt% CB or 5 wt% CB + 2.5 wt% CNF. Although the total amount of conductive additives is not equal in the two cases, we will show that our method still allows the comparison to be done.

3. Experimental

3.1. Materials

$LiFePO_4$ was prepared by mechanochemistry using commercial Li_3PO_4 and fresh iron (II) phosphate as the source of the main components, together with the electronic conductor additive precursor (sucrose for carbon coating). The powders were ball milled in a planetary mill (Retsch S1000) with agate vessels. The resulting product was then heat-treated at 550 °C under nitrogen for 15 min to crystallize the final compound $LiFePO_4$ with the desired coating around the particles. This active material is mixed with several additives to form the electrode slurry. Carbon Super P (specific surface of 60 m^2 g^{-1}, Timcal), hereafter named CB, and Vapor Grown Carbon Fibers, hereafter named VGCF (diameter 100–200 nm and length 5–20 μm, Showa Denko), chosen as conductive additives, were incorporated in aqueous slurries using a nonionic surfactant (Triton X-100 from Aldrich). Butadiene–acrylonitrile copolymer rubber latex (NBR from PolymerLatex) was used as the binder and CMC (0.7 carboxyl unit per molecule cellulose (DS = 0.7), Mw = 250 000 g mol^{-1}, Aldrich) as the thickening agent.

3.2. Preparation of the composite electrode

Electrode slurries were prepared in deionized (DI) water at a solid fraction of 23 wt% with a high-speed mixer used to shear the electrode slurry for 5 min. The slurry was then tape-casted by using an automatic doctor blade onto an aluminum current collector. The gap between the blade and the current collector was fixed from 100 μm to 1000 μm resulting in electrode loadings in the range of 0.4–3.7 mAh cm^{-2} surface capacity. Drying is done at 55 °C to remove water and electrodes are then densified to adjust their porosity. Before battery assembly, an additional drying at 80 °C under dynamic vacuum is performed. The electrode compositions were 87.5 wt% $LiFePO_4$, 5 wt% CB, 1.5 wt% TX100, 2 wt% CMC, 4 wt% NBR or 85 wt% $LiFePO_4$, 5 wt% CB + 2.5 wt% VGCF, 1.5 wt% TX100, 2 wt% CMC, and 4 wt% NBR.

3.3. Battery assembly and characterization

$LiFePO_4$-based composite electrodes are assembled in electrochemical cells with lithium metal as counter electrode, Celgard film as a separator soaked in an electrolyte consisting of a 1 M $LiPF_6$ solution in an ethylene carbonate–diethyl carbonate (EC–DEC 1/1) mixture. The button cells assembly is carried out in a dry glove box under argon atmosphere. Electrochemical experiments are performed at 20 °C and monitored by an Arbin instrument, between 2.0 and 4.2 V versus Li^+/Li.

3.4. Electrode electrical properties

The electronic resistance measurements were carried out by impedance spectroscopy on dry $LiFePO_4$ electrode/current collector samples sandwiched in between two metallic plungers in a standard swagelok cell. The value of R_e the dry electrode transverse electronic resistance enables to determine ρ_e the apparent electronic resistivity of the electrode via the equation: $R_e = \rho_e L/S$, where L and S are respectively the thickness and the surface of the electrode analyzed.

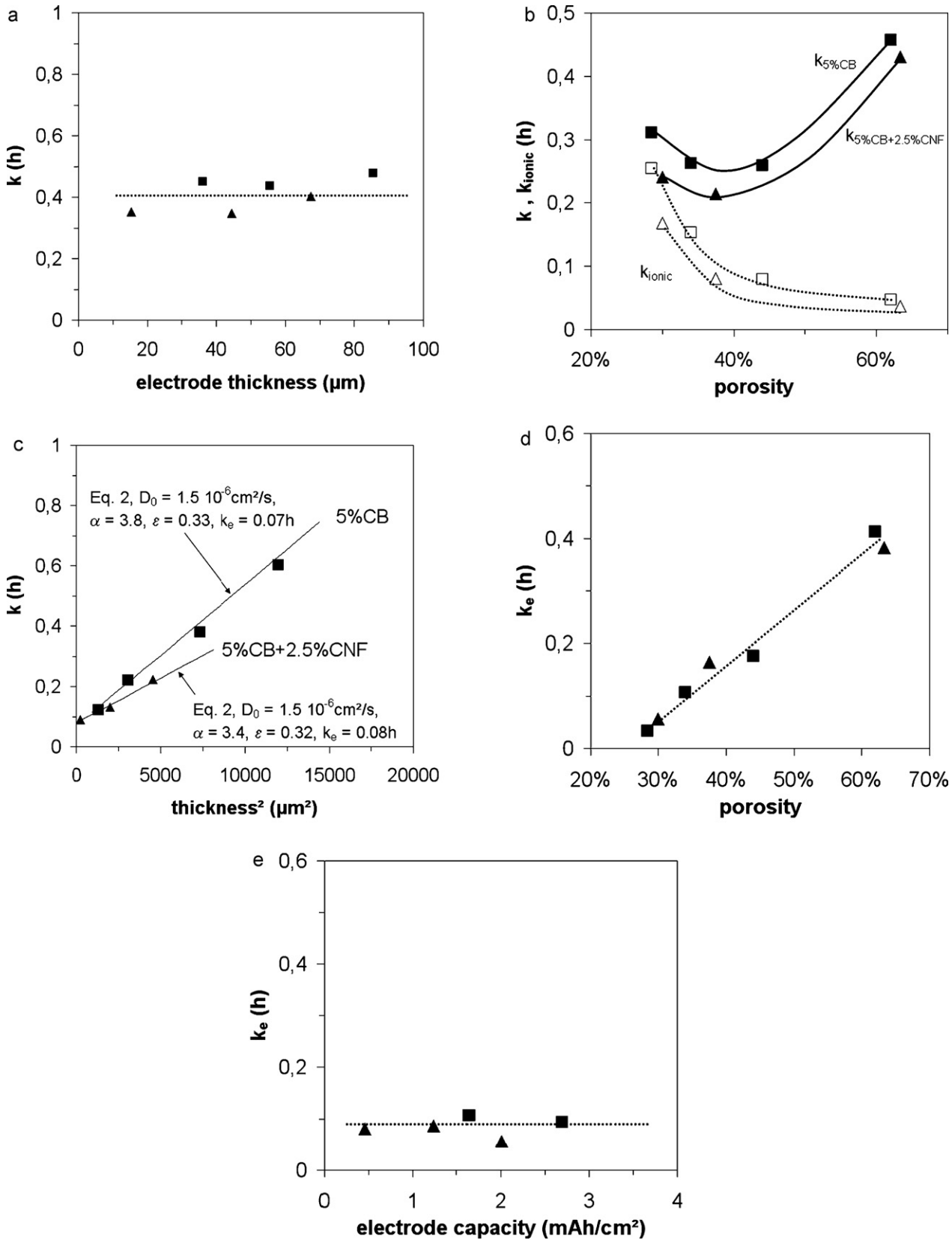

Fig. 3. For electrodes containing 5 wt% (■, □) or 7.5 wt% (▲, △) of conductive additives: (a) k as a function of the electrode thickness for rates in the $C/50$–$C/10$ range – 32% of porosity; (b) k (full symbols) and k_{ionic} (open symbols) as functions of the electrode porosity for rates in the $C/10$–$2C$ range and for 1.9 mAh cm^{-2} electrodes; (c) k as a function of the square of the electrode thickness for rates in the $C/10$–$2C$ range – 32% of porosity; (d) k_e as a function of the electrode porosity for 1.9 mAh cm^{-2} electrodes for rates in the $C/10$–$2C$ range; and (e) k_e as a function of the electrode capacity – 32% of porosity for rates in the $C/10$–$2C$ range.

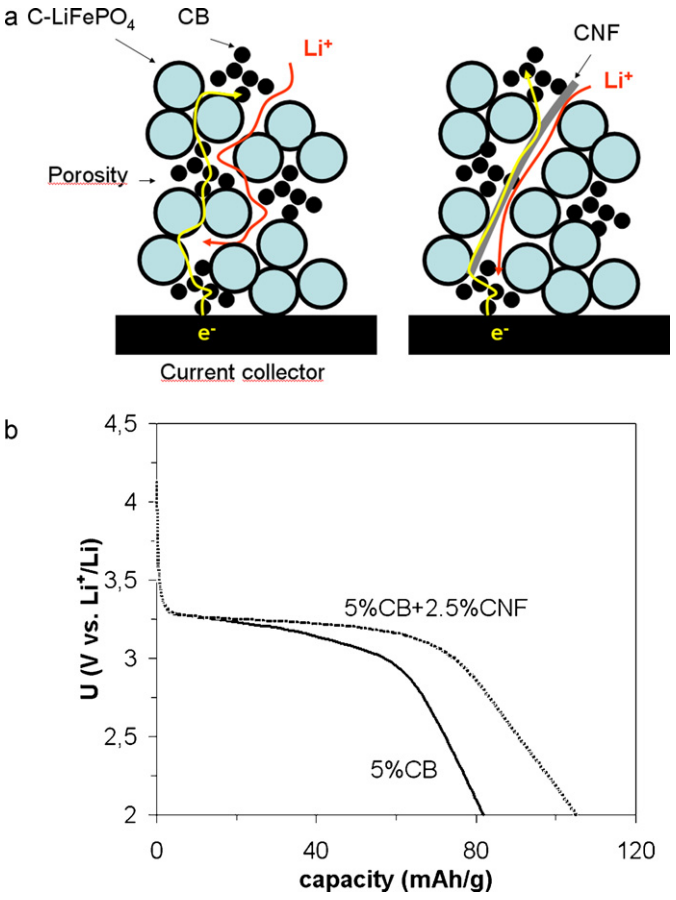

Fig. 4. (a) Schematic description of the composite electrode architecture, with and without CNF, and the relationships with the parameters of our model. (b) Discharge curves for ~2 mAh cm^{-2}, 35–40% porosity, $LiFePO_4$-based electrodes of containing 5 wt% (solid lines) or 7.5 wt% (dotted lines) of conductive additives at the *C* rate.

4. Results

4.1. Morphological/textural study

$LiFePO_4$ is in the form of primary particles, with a diameter in the 60–100 nm range, fused into secondary particles with a mean diameter of 20 μm. The large $LiFePO_4$ agglomerates are well distributed within a homogeneous matrix of small $LiFePO_4$ and CB agglomerates (Fig. 1a and c). The binders form a thin continuous amorphous layer covering the surfaces of $LiFePO_4$ and CB particles and they bridge together $LiFePO_4$ and CB particles [14,16,17]. When CNF are added, they are well dispersed in the matrix (Fig. 1b and d).

The dry electronic resistivity ρ_e (evaluated from a two probe measurement) and R_w are compared in Fig. 2 for the two conductive additive compositions as a function of the total porosity of the composite electrode (Fig. 2a) or as a function of the conductive additive total volume fraction $\phi_{CB} + \phi_{CNF}$ (Fig. 2b). The volume fraction of the i constituent ϕ_i was calculated from the well known formula: $\phi_i = \%w_i \times \rho_{app,e}/\rho_i$ where $\%w_i$ and ρ_i are the weight fraction and the bulk density (g cm^{-3}) of the i constituent, respectively, and $\rho_{app,e}$ is the apparent density of the electrode determined according to $\rho_{app,e} = m_e/(e_e \times S_e)$, where m_e, e_e and S_e are the mass, the thickness and the surface of the electrode, respectively.

In Fig. 2a, one can see that R_w and ρ_e vary the same way, confirming the origin of R_w (resistance of the electronic wires of the better connected active material grains). The diminution of both properties when the porosity is decreased results from the increase of the conductive additive volume fraction (Fig. 2b), and the improvement of contacts between particles and at the interface with the current collector upon calendaring of the composite electrode. Moreover, with the addition of CNF, electrons must transfer through much less numerous inter-particle contacts due to the fibers length which results in improved electronic conductivity. At porosities below 35%, which corresponds to $\phi_{CB} + \phi_{CNF}$ superior to ~5%, one can note that R_w is somewhat independent of the conductive additive mix and levels at a value of about 20 Ω, although ρ_e is notably decreased with the addition of CNF by a factor of about 2. R_w quantifies the contribution of electronic wires to the electrode resistance at low lithium insertion degree and thus characterizes the wires of the better-connected active particles (that insert lithium first). From Fig. 2, it can be concluded that for porosities below 35%, corresponding to well-densified composite electrodes, adding CNF to the conductive additives mix results in almost no improvement of the electronic wiring of the better-connected AM particles. R_w gathers (i) the contact resistance at the current collector/electrode interface, (ii) the inter-particle contact resistances between conductive additives (iii) and between these ones and the AM particles, and finally (iv) the resistance of the carbon coating that surrounds each AM particle. The lack of variation of R_w for well-densified composite electrodes can be interpreted in two different ways: (i) the densification allows to reduce enough inter-particle resistances so that electrons can transport very easily into the CB percolated network with negligible resistance [13]; (ii) better connected AM particles are close to the current collector and thus their wiring is not very much dependent on the presence of long conductive fibers [18].

Poorly connected AM particles react at lower potential due to increased polarization, which is captured in our model by the term R_x. Fig. 2c shows R_x for the two compositions as a function of the electrode capacity in the 30–35% porosity range. When CNF are added, a much lower value of R_x is observed for thick electrodes (for example at 2 mAh cm^{-2}), while no effect is observed for thin electrodes. This suggests that adding CNF results in more homogeneous and efficient electronic and/or ionic wiring of poorly connected AM particles in the case of thick electrodes. Some clarification can be obtained by looking at the rate factor *k*.

The general features of the rate factor are not modified by adding the CNF (Fig. 3). *k* was found to be independent on the electrode composition and on the active mass loading (or thickness) for rates in the *C*/50–*C*/10 range, Fig. 3a. Actually at these low rates, there is no kinetic limitation from the composite electrode wires, and *k* is thus only dominated by the solid-state mass transport into the bulk of the active grains [14]. For rates in the *C*/10–2*C* range, *k* is found to depend on the composite electrode porosity, Fig. 3b, and thickness, Fig. 3c. Moreover, as already observed and discussed in the background section, *k* is lower at high rate than at low rate [14]. At rates in the *C*/10–2*C* range, we are thus left only with the contribution of the composite electrode framework, and *k* can be written.

$$k = \frac{L^2}{3D_0\varepsilon^\alpha} + k_e(L, \varepsilon) \quad (7)$$

The dependence of *k* on the electrode porosity (Fig. 3b) traduces the compromise between ionic and electronic wirings of the active mass, the former being optimized at high porosity and the latter being optimized at low porosity (in the 30–35% range). Below the range of porosity where *k* is minimized (35–40% range), *k* is dominated by ionic wiring limitations highlighted by the dependence of *k* on the square of the electrode thickness (Fig. 3c) [14].

In the 30–35% porosity range, k_e can be considered a constant term independent on *L* and ε [14], and the linear fit of *k* with L^2 (Eq. (7)) allows to get α, the tortuosity factor, using the experimental values of *L* and ε and tabulated value for D_0, 1.5×10^{-6} cm^2 s^{-1} [19] (Fig. 3c). α is found to be 3.8 when the electrode only contains CB

as conductive additive and 3.4 when CNF are added. The lower α tortuosity value got for the composite electrode with CNF can be attributed to the fibers that create some 1D channel along their length, thereby decreasing the electrode tortuosity and favoring the lithium ion diffusion [20]. In addition to a favored tortuosity, Li^+ ionic mobility could be enhanced along the fibers through adsorbed Li^+ ion.

The difference between the experimental value of k and the calculated value of k_{ionic} is k_e, the electronic limitation to the rate factor (Eq. (7)). The latter is found roughly invariant with the addition of CNF (Fig. 3d and e). Common sense would expect a decrease of k_e with the addition of CNF, as observed for R_w, but the composite electrodes architecture should be kept in mind: the AM particles are in the form of clusters. Particles from the clusters shell are point contacted with the electronic network formed by the conductive additive/binder mixture while particles into the core of the clusters, which represent the majority of the active mass, are electronically wired through the carbon coating. The invariance of k_e with the addition of CNF might reveal that the carbon coating dominates the electronic limitations of the rate performance. Another interpretation is that what ultimately dominates k_e is the contact resistance at the current collector interface, likely independent on the addition of CNF [21,22].

The improvement brought here by using some CNF is illustrated in Fig. 4 where the composite electrode architecture is schematized and the discharge curves at the C rate of composite electrodes in the optimal porosity range are shown. In agreement with the main findings of this work for optimized porosity, this scheme shows a similar electronic wiring, but an improved ionic wiring due to enhanced shape factor of the fibers.

5. Conclusion

The use of carbon nanofibers (CNF) in carbon coated $LiFePO_4$-based composite electrodes leads to an improvement of the electrochemical performance at high rate. We show here that CNF favor a more homogeneous supply of electrons to the active mass which results in a lower polarization in case of non-optimized porosity. For optimized porosity, no better electronic wiring is achieved, but these CNF also improve the composite electrode ionic conductivity thanks to their fibrous shape that allows lowering the tortuosity of the pores and thus enhances the ions transport in the whole composite electrode. Due to their unique combination of shape and mechanical properties, CNF offer possibilities to build new more efficient composite electrode architectures. In the future work, we will focus on the cyclability of the composite electrodes prepared with CNF. As a matter of examples, in the literature, both an improvement and a degradation of the cyclability of silicon-based negative electrodes have been observed [2,3].

Acknowledgments

C.F. gratefully acknowledges ADEME (Agence De l'Environnement et de la Maîtrise de l'Energie) and CEA/INSTN (Commissariat à l'Energie Atomique et aux Energies Alternatives/Institut National des Sciences & Techniques Nucléaires) for financial support of her PhD.

References

[1] M. Endo, Y.A. Kim, T. Hayashi, K. Nishimura, T. Matusita, K. Miyashita, M.S. Dresselhaus, Carbon 39 (2001) 1287.
[2] B. Lestriez, S. Desaever, J. Danet, P. Moreau, D. Plée, D. Guyomard, Electrochem. Solid-State Lett. 12 (2009) A76.
[3] J. Guo, A. Sunn, X. Chen, C. Wang, A. Manivannan, Electrochim. Acta 56 (2011) 3981.
[4] F. Mizuno, A. Hayashi, K. Tadanaga, M. Tatsumisago, J. Electrochem. Soc. 152 (2005) A1499.
[5] M.S. Wu, J.T. Lee, P.C.J. Chiang, J.C. Lin, J. Mater. Sci. 42 (2007) 259.
[6] J.T. Lee, Y.J. Chu, F.M. Wang, C.R. Yang, C.C. Li, J. Mater. Sci. 42 (2007) 10118.
[7] Y.B. Yi, C.W. Wang, A.M. Sastry, J. Electrochem. Soc. 151 (2004) A1292–A1300.
[8] M. Gaberscek, J. Jamnik, Solid State Ionics 177 (2006) 2647.
[9] D. Guy, B. Lestriez, R. Bouchet, V. Gaudefroy, D. Guyomard, Electrochem. Solid-State Lett. 8 (2005) A17.
[10] G. Liu, H. Zheng, S. Kim, A.S. Simmens, A.M. Minor, X. Song, V.S. Battaglia, J. Electrochem. Soc. 154 (2007) A1129.
[11] D.H. Jang, S.M. Oh, Electrochim. Acta 43 (1998) 1023.
[12] R. Dominko, M. Gaberscek, J. Drofenik, M. Bele, S. Pejovnik, Electrochem. Solid-State Lett. 4 (2001) A187–A190.
[13] D. Guy, B. Lestriez, R. Bouchet, D. Guyomard, J. Electrochem. Soc. 153 (2006) A679.
[14] C. Fongy, A.C. Gaillot, S. Jouanneau, D. Guyomard, B. Lestriez, J. Electrochem. Soc. 157 (2010) A885.
[15] C. Fongy, S. Jouanneau, D. Guyomard, J.-C. Badot, B. Lestriez, J. Electrochem. Soc. 157 (2010) A1347.
[16] W. Porcher, B. Lestriez, S. Jouanneau, D. Guyomard, J. Electrochem. Soc. 156 (2009) A133.
[17] W. Porcher, B. Lestriez, S. Jouanneau, D. Guyomard, J. Power Sources 195 (2010) 2835.
[18] V. Srinivasan, J. Newman, J. Electrochem. Soc. 151 (2004) A1517.
[19] S.G. Stewart, J. Newman, J. Electrochem. Soc. 155 (2008) F13.
[20] W. Lai, C. Erdonmez, T. Marinis, C. Bjune, N. Dudney, F. Xu, R. Wartena, Y.-M. Chiang, Adv. Mater. (Weinheim) 22 (2010) 139.
[21] M. Gaberscek, J. Moskon, B. Erjavec, R. Dominko, J. Jamnik, Electrochem. Solid-State Lett. 11 (2008) A170.
[22] H.-C. Wu, H.-C. Wu, E. Lee, N.-L. Wu, Electrochem. Commun. 12 (2010) 488.